Hydrogen Storage Materials

Deutsche Ausgabe: DOI: 10.1002/ange.201605961
Internationale Ausgabe: DOI: 10.1002/anie.201605961

Dehydrogenation of Formic Acid at Room Temperature: Boosting Palladium Nanoparticle Efficiency by Coupling with Pyridinic-Nitrogen-Doped Carbon

*Qing-Yuan Bi, Jian-Dong Lin, Yong-Mei Liu, He-Yong He, Fu-Qiang Huang, and Yong Cao**

Abstract: *The use of formic acid (FA) to produce molecular H_2 is a promising means of efficient energy storage in a fuel-cell-based hydrogen economy. To date, there has been a lack of heterogeneous catalyst systems that are sufficiently active, selective, and stable for clean H_2 production by FA decomposition at room temperature. For the first time, we report that flexible pyridinic-N-doped carbon hybrids as support materials can significantly boost the efficiency of palladium nanoparticle for H_2 generation; this is due to prominent surface electronic modulation. Under mild conditions, the optimized engineered $Pd/CN_{0.25}$ catalyst exhibited high performance in both FA dehydrogenation (achieving almost full conversion, and a turnover frequency of 5530 h^{-1} at 25 °C) and the reversible process of CO_2 hydrogenation into FA. This system can lead to a full carbon-neutral energy cycle.*

The replacement of conventional fossil fuels with a clean CO_2-neutral energy cycle is a key global challenge.[1] Hydrogen is a promising energy carrier that has been largely used in fuel-cell-based technology.[2] However, its safe storage and transport remain significant bottlenecks to wider use as a fuel.[3] Formic acid (HCOOH or FA), is a safe and convenient hydrogen carrier, which has been extensively applied in renewable energy storage because of its considerable hydrogen content (4.4 wt%), nontoxicity, liquid state, easy accessibility, and high stability under ordinary conditions.[2,4] More importantly, the gravimetric energy density of FA is seven times higher than that of the commercially available lithium-ion batteries.[5] FA decomposition may occur by two distinct reaction pathways, either by decarboxylation (Equation 1), or dehydration (Equation 2).[6]

$$HCOOH \rightarrow H_2 + CO_2 \quad (1)$$

$$HCOOH \rightarrow H_2O + CO \quad (2)$$

[*] Dr. Q. Y. Bi, J. D. Lin, Dr. Y. M. Liu, Prof. Dr. H. Y. He, Prof. Dr. Y. Cao
Department of Chemistry, Shanghai Key Laboratory of Molecular Catalysis and Innovative Materials, Collaborative Innovation Center of Chemistry for Energy Materials, Fudan University
Shanghai 200433 (P.R. China)
E-mail: yongcao@fudan.edu.cn
Dr. Q. Y. Bi, Prof. Dr. F. Q. Huang
State Key Laboratory of High Performance Ceramics and Superfine Microstructures, Shanghai Institute of Ceramics
Chinese Academy of Sciences
Shanghai 200050 (P.R. China)

Supporting information for this article can be found under: http://dx.doi.org/10.1002/anie.201605961.

For FA to be usable as a H_2 carrier, it is essential that only the first reaction takes place, to achieve the maximum possible H_2 formation and to avoid the presence of toxic CO. CO_2 is an ideal C_1 building block and hydrogen vector that can be hydrogenated to form FA (Equation 3).[7]

$$H_2 + CO_2 \rightarrow HCOOH \quad (3)$$

In this way a full carbon-neutral energy cycle can be obtained.

The dehydrogenation of FA with homogeneous catalysts has been widely investigated.[8] However, the use of various additives and/or organic solvents tends to limit their practical large-scale application. Some of the drawbacks associated with homogeneous catalysts are largely mitigated in solid catalysts.[9,10] Among the heterogeneous catalysts, many active components have been shown to be effective for H_2 evolution by FA decomposition because of the simple handling and significant reusability associated with heterogeneous materials.[9,10] However, despite their high performance most reaction processes need the addition of alkali compounds (sodium or potassium salts, or organic amines), which can lower the gravimetric energy density of FA.[9a,f–i,10a] The development of a FA system without any additives would be advantageous to maximize the overall deliverable capacity of FA.[9d,e,j–m,10b] This would also be beneficial to the quality of the H_2 gas released. In fact, ultraclean H_2 could be used in direct downstream applications in fuel-cell-based technologies for clean power generation.[5,10b] For all of these reasons, it is highly desirable to develop a heterogeneous catalyst that is simple, efficient, and robust, thereby allowing selective production of ultrapure H_2 gas from FA. Ideally, the catalyst should work in a base-free aqueous medium under ambient conditions.

Palladium metal is a common active component in aqueous FA decomposition at low temperatures and in base-free conditions.[9e,j] However, the poor H_2 selectivity and intrinsically weak CO tolerance of Pd can lead to reduced stability of the metal. Hence, tremendous efforts have been devoted to solving these issues; possible solutions include alloys and core–shell structures.[9d,k,l] However, the preparation methods are difficult to control and the catalytic activities need further improvement. An alternative to this strategy is to modify the surface electronic structure of the supported Pd catalyst with underlying flexible materials (for example, carbon-based supports). A modulated electronic structure of carbon-supported Pd nanoparticles (NPs) could serve as a new and effective way to boost efficiency. A crucial feature, which is still unresolved, is the precise control of surface properties of the Pd NPs. Herein, for the first time, we present

an efficient and reliable process involving electron-rich pyridinic-N addition into the carbon hybrid; we used a chemical method that can effectively modulate the surface electronic and acid–base properties of the Pd catalyst, and thus enhance its catalytic performance. In comparison to existing catalysts, the engineered pyridinic-N-tuned Pd catalyst showed great improvements in terms of catalytic activity and durability toward FA dehydrogenation and CO_2 hydrogenation.

We began our research by synthesizing a series of CN_x (where x denotes the N/C molar ratio based on elemental analysis data) with a bio-chitosan-based pyrolysis strategy; this was done by using a combination of chitosan and melamine, following the reported procedure.[11] The obtained materials were then loaded with approximately 10 wt % of Pd by a wet chemical reduction method.[10b] A well-defined linear array of mesoporous structures and nanosheet-like morphology were observed for materials with the formulae $CN_{0.15}$, $CN_{0.23}$, $CN_{0.39}$, $CN_{0.62}$, and $CN_{0.95}$ (Supporting Information, Figure S1 and Table S1). Typical TEM images demonstrate that Pd NPs with an average size of 3.2 ± 0.3 nm were uniformly dispersed on the N-doped carbon supports (Supporting Information, Figure S3). XPS results show that Pd had a negative charge; this indicates a possible electron transfer from CN_x to Pd NPs (Supporting Information, Figure S4). The effect of the CN_x supports on the charge of the Pd NPs was further investigated with ATR-IR spectroscopy,[9e] by monitoring the adsorbed linear mode of CO on Pd/CN_x (Figure 1 a). Nitrogen addition results in a lower wavenumber than for the undoped counterpart; the extent of the red shift was higher for samples with higher N content in the CN_x materials. These data confirm that CN_x supports have a strong electronic effect on Pd NPs, depending on the N content.

The catalytic properties of the Pd/CN_x catalysts for FA dehydrogenation were evaluated in a base-free aqueous medium (1M FA) and in mild conditions (25 °C). For this overall decarboxylation process, the adsorption of the FA molecules and the cleavage of the O–H bond can be promoted by modified surface Lewis base properties because of the presence of the N dopant. The following key step of the C–H bond cleavage can be effectively chemically catalyzed by the modulated Pd NPs on the surface of the electronic structure.[9e] A plot of activity as a function of the N content of the Pd/CN_x catalysts did not show a linear correlation. In fact, $Pd/CN_{0.95}$ showed the strongest electronic effect between Pd NPs and N-doped support but corresponded to the lowest performance, while $Pd/CN_{0.23}$ presented the highest TOF (Supporting Information, Figure S5). To better understand this phenomenon, we carried out further characterization. Based on XPS analysis of the N 1s and of the surface metal compositions, we found that there are three different N states (graphitic-, pyrrolic-, and pyridinic-N),[11,12] as shown in Figure S6 (Supporting Information). Pyridinic-N was shown to be the main contributor to the electronic interaction with Pd NPs, and the surface pyridinic-N/Pd molar ratio was responsible for the catalytic activity (Figure 1 b). This is in line with the previous demonstrations of Pt-based catalysis.[13] Remarkably, $Pd/CN_{0.23}$ was found to be highly active for FA decomposition, with an impressive turnover frequency (TOF)

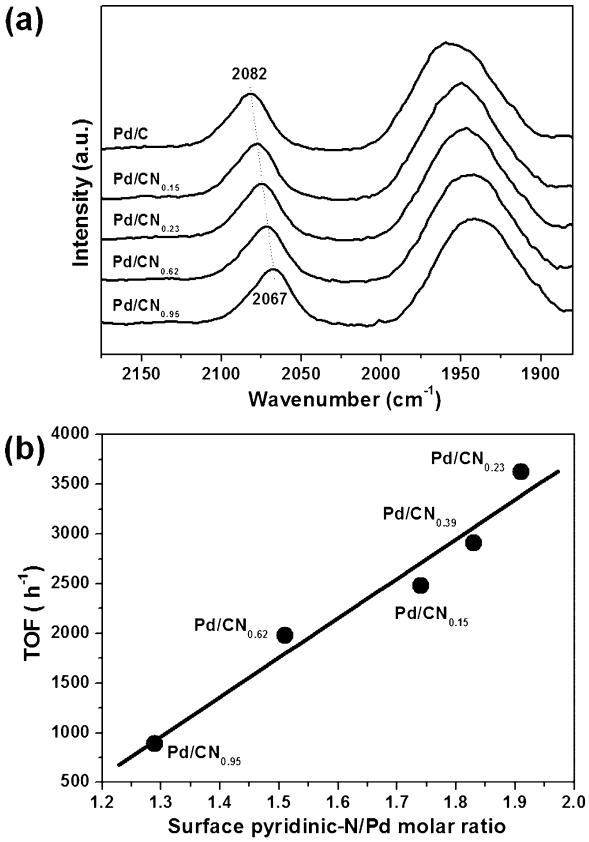

Figure 1. a) ATR-IR of CO on Pd/CN_x catalysts. b) Correlation between the surface pyridinic-N/Pd molar ratio and the initial TOF value of Pd/CN_x catalysts.

of $3625\ h^{-1}$ per surface Pd site (Supporting Information, Figure S5); the catalyst was selective, forming equivalent amounts of H_2 and CO_2.

To verify and understand the effect of the surface pyridinic-N, we modified commercial composite Pd-based catalysts with N-containing model organic molecules (Supporting Information, Table S3). Modification with pyrrole decreased the performance, while pyridine and 3-aminopyridine improved the activity of both Pd catalysts. These results confirm that pyridinic-N beneficially modulates the electronic properties of the Pd catalyst surface, thereby promoting H_2 generation. Therefore, we prepared various N-doped carbons (NDCs) with the general bio-chitosan-based pyrolysis strategy; a family of N- and/or C-containing chemicals, such as polyethyleneimine, urea, peptone, and acetonitrile, were used. The N/C molar ratio of the formed materials was maintained at 0.25 ± 0.1 by changing the weight of precursors used (Supporting Information, Table S4).[14] Results in Figure S7 (Supporting Information) and images in Figures 2 a,b and Figure S8 (Supporting Information) clearly show the mesoporous nature and the nanosheet-like structure of these samples. For the supported catalysts, Pd NPs with average sizes of 3.0 to 3.5 nm were uniformly dispersed on supports. Notably, the sample that combined chitosan and urea supported Pd NPs of 3.1 ± 0.3 nm (Figure 2 c) demonstrated a higher specific surface area of $465\ m^2 g^{-1}$ (Supporting Information, Figure S7). HAADF-

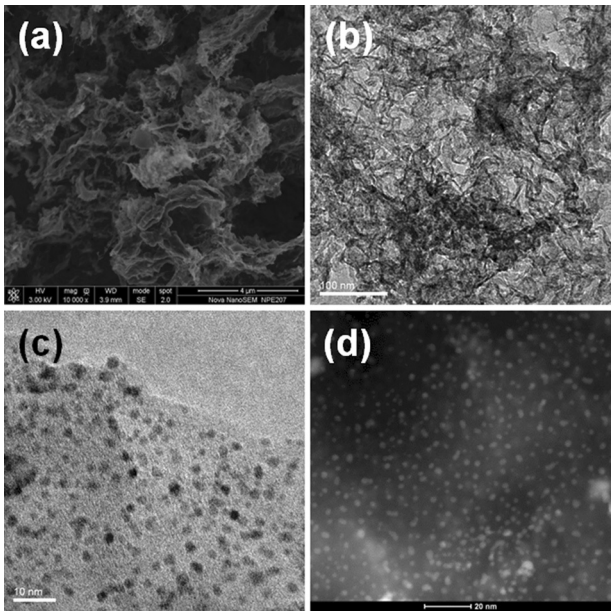

Figure 2. a) FESEM and b) TEM images of $CN_{0.25}$ material. c) TEM and d) HAADF-STEM images of $Pd/CN_{0.25}$ catalyst.

STEM and TEM images (Figures 2d; Supporting Information, Figure S9) showed the Pd NPs were distinctly anchored on the underlying supports. Moreover, the surface of Pd NPs obviously possessed a negative charge because of the electronic interaction between metal and N-doped carbon hybrids (Supporting Information, Figure S10).

These NDC-supported Pd catalysts were then tested for FA dehydrogenation. To our delight, $Pd/CN_{0.25}$ displayed the highest ever reported activity of 5530 h^{-1} at 25 °C (Supporting Information, Table S4 and Figure S11).[9,10] For the supported Pd catalysts with identical metal loading and similar particle size, the lattice microstrains resulting from the lattice mismatch between Pd and the underlying support are negligible (Supporting Information, Figure S12).[10b] On the basis of elemental analysis and XPS spectra of N 1s (Supporting Information, Table S5), an excellent and positive linear correlation could be seen between the catalytic activity and the surface pyridinic-N/Pd molar ratio (Supporting Information, Figure S13); this is consistent with the results for supported Pd systems made from chitosan and melamine (Figure 1b). These data indicate that the Pd NPs can be strongly modified with the electronic effect of NDCs—especially by the surface pyridinic-N. This effect can induce unique surface chemical properties in the Pd catalyst and lead to high FA dehydrogenation performance.

In the microenvironment of Pd NPs, an excess of pyridinic-N may induce stronger adsorption of formate intermediates; this can result in a decrease in the catalytic activity (Supporting Information, Table S6). A Pd loading of 10 wt% on $CN_{0.25}$ was beneficial to the metal–support electronic interaction and surface metal atomic density, as shown in Figure S16 (Supporting Information). Control experiments with Pd-free $CN_{0.25}$ show that the presence of Pd was essential to achieve high FA dehydrogenation activity (Supporting Information, Table S7). A comparison with Au, Pt, Ru, Rh, and Ir NPs supported on $CN_{0.25}$ as reference catalysts (Supporting Information, Figure S17) showed that Pd is uniquely active on the N-doped carbon materials for selective FA decomposition (Supporting Information, Table S7). In contrast to the catalysts in which Pd with an identical metal loading (10 wt%) is supported on conventional metal oxides and reduced graphene oxide (rGO),[10b] the $Pd/CN_{0.25}$ hybrid exhibited the highest activity toward FA decomposition into H_2 (Supporting Information, Table S7). Note that a previously reported catalyst of Pd/mpg-C_3N_4 with a metal particle size of 3.0 ± 0.2 nm (Supporting Information, Figure S18)[15] showed a much lower activity (1247 h^{-1}).

The dependence of the FA concentration and reaction temperature on the dehydrogenation rate of FA over a $Pd/CN_{0.25}$ was also studied. The rates of H_2 release increased as the FA concentration increased from 0.5 to 1.0 M (Supporting Information, Figure S19). However, higher values were found to have a negative effect on dehydrogenation kinetics. Despite the reduced activities at concentrations higher than 1.0 M, the catalyst still showed enhanced activity compared to previous results, even at concentration as high as 4.0 M.[9d,e,j–l] This represents a clear advantage for practical applications. Moreover, 240 mL of gas can be readily generated within 1 h over $Pd/CN_{0.25}$ at 25 °C (Figure 3), corresponding to almost full conversion (up to 97.5%) of FA into H_2 and CO_2. It is also important to highlight that in all catalytic experiments, ultraclean H_2 gas was generated without the detection of toxic CO, which is essential to enable direct downstream applications in fuel-cell-based technologies for clean power generation in a modern hydrogen economy.[5,10b,16] The reaction rate was higher at higher temperatures, but even at lower temperatures a significant H_2 evolution (TOF up to 1449 h^{-1} at 10 °C) can still be obtained (Figure 3). The apparent activation energy (E_a) was estimated to be 48.8 kJ mol^{-1} (Supporting Information, Figure S21), which is lower than that determined for the previously reported heterogeneous catalysts.[9a,10a,17]

Additionally, the heterogeneous nature and reusability of this catalytic system was confirmed by the following results.

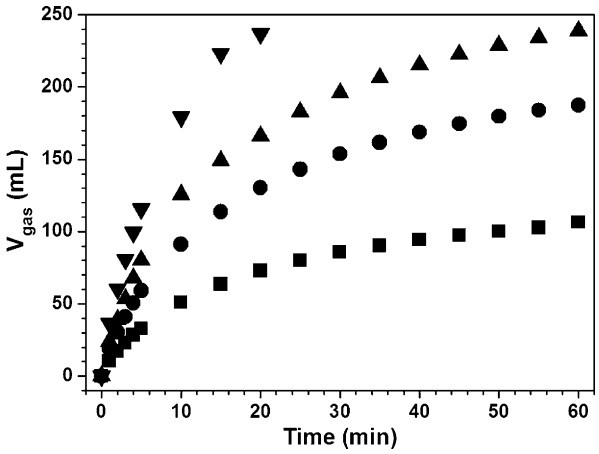

Figure 3. H_2 evolution by FA decomposition catalyzed by $Pd/CN_{0.25}$ catalyst at different temperatures. Reaction conditions: aqueous FA (1 M, 5.0 mL scale), Pd (37.7 μmol); 10 °C (■), 20 °C (●), 25 °C (▲), 35 °C (▼).

$Pd/CN_{0.25}$ was removed from the reaction mixture at half FA conversion. Further processing of the filtrate at 25 °C for 1 h did not increase the conversion. Inductively coupled plasma atomic emission spectroscopy (ICP-AES) analysis of the filtrate showed that the content of Pd in the solution was below the detection limit. These data confirmed that the reaction is attributed to the heterogeneous catalysis of $Pd/CN_{0.25}$. This catalyst retains excellent stability for large scale H_2 release; an overall stream of 4.4 L of gas, corresponding to a 90% conversion, can be readily attained from 100.0 mL of 1.0 M FA within 600 min (Figure 4). As shown in the inset to Figure 4, the catalyst was reused up to six times without significant loss of catalytic efficiency; the 50040 total turnover number (TON) reached the highest value yet reported in clean heterogeneous systems, thus further demonstrating the effectiveness of $Pd/CN_{0.25}$ at room temperature. Furthermore, the $Pd/CN_{0.25}$ catalyst showed unique robustness and was air stabile for half a year in ambient conditions (Supporting Information, Figure S23).

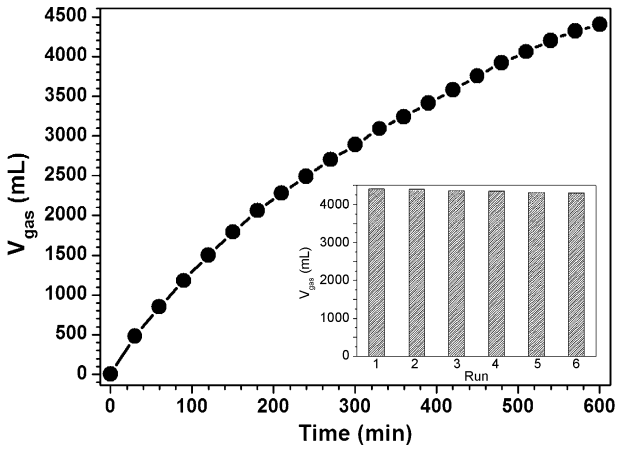

Figure 4. Large scale H_2 generation from FA over $Pd/CN_{0.25}$ catalyst. The inset shows the durability of $Pd/CN_{0.25}$. Reaction conditions: aqueous FA (1 M, 100.0 mL scale), Pd (75.4 μmol), 25 °C, 600 min.

These promising results prompted us to evaluate $Pd/CN_{0.25}$ in the reverse reaction; that is, FA formation by hydrogenation of CO_2.[10b,16,18] The Pd catalyst displayed a high FA yield and TON values (up to 97.2% and 135074, respectively; Supporting Information, Table S8). This is the best performance reported for heterogeneous catalysts under relatively mild conditions,[10b,18a] and is comparable to most values obtained with organic complexes.[16,19] The high efficiency of this $Pd/CN_{0.25}$ catalyst can be reasonably attributed to enhanced electron modulation of the catalyst surface. Modern industrial technology offers a variety of appropriate methods for the realization of large scale FA separation and extraction from CO_2-containing products. Therefore, in the presence of an efficient $Pd/CN_{0.25}$ catalyst, FA can be selectively decomposed to H_2 and CO_2, and a carbon-neutral cycle can also be obtained by recycling the CO_2 back to FA.

In conclusion, the most significant advances in the design of Pd/CN_x catalysts for base-free aqueous FA dehydrogenation at room temperature have mainly focused on the incorporation of active Pd NPs on a matrix of flexible pyridinic-N-doped carbon hybrids. By employing a controlled synthetic approach involving a bio-chitosan-based pyrolysis strategy, we have demonstrated that a further and complementary optimization of Pd NPs can be achieved by a simple surface electronic modulation with the pyridinic-N group. This method leads to an enhancement of FA dehydrogenation catalytic efficiency as well as CO_2 hydrogenation. The present findings can make a significant contribution, not only in terms of disclosing the electron-rich pyridinic-N-tuned Pd catalyst as a means to boost catalytic efficiency, but also to establish a viable and convenient H_2 production process with a carbon-neutral cycle for clean and sustainable energy storage.

Acknowledgements

This work was supported by NSF of China (21273044, 21473035, 91545108, and 51502331), Science & Technology Commission of Shanghai Municipality (16ZR1440400), and the Open project of State Key Laboratory of Chemical Engineering (SKL-ChE-15C02).

Keywords: formic acid · heterogeneous catalysis · hydrogen storage · Pd nanoparticles · pyridinic-N-doped carbon

How to cite: *Angew. Chem. Int. Ed.* **2016**, *55*, 11849–11853
Angew. Chem. **2016**, *128*, 12028–12032

[1] a) U. Eberle, M. Felderhoff, F. Schüth, *Angew. Chem. Int. Ed.* **2009**, *48*, 6608; *Angew. Chem.* **2009**, *121*, 6732; b) M. Aresta, A. Dibenedetto, A. Angelini, *Chem. Rev.* **2014**, *114*, 1709.
[2] a) S. Enthaler, *ChemSusChem* **2008**, *1*, 801; b) F. Joó, *ChemSusChem* **2008**, *1*, 805; c) X. Liu, S. S Li, Y. M. Liu, *Chin. J. Catal.* **2015**, *36*, 1461.
[3] a) L. Schlapbach, A. Züttel, *Nature* **2001**, *414*, 353; b) *Handbook of Hydrogen Storage* (Ed.: M. Hirscher), Wiley-VCH, Weinheim, **2010**; c) Q. L. Zhu, Q. Xu, *Energy Environ. Sci.* **2015**, *8*, 478.
[4] T. C. Johnson, D. J. Morris, M. Wills, *Chem. Soc. Rev.* **2010**, *39*, 81.
[5] A. Boddien, C. Federsel, P. Sponholz, D. Mellmann, R. Jackstell, H. Junge, G. Laurenczy, M. Beller, *Energy Environ. Sci.* **2012**, *5*, 8907.
[6] H. Dai, B. Xia, L. Wen, C. Du, J. Su, W. Luo, G. Cheng, *Appl. Catal. B* **2015**, *165*, 57.
[7] a) S. Enthaler, J. Langermann, T. Schmidt, *Energy Environ. Sci.* **2010**, *3*, 1207; b) *Carbon Dioxide as Chemical Feedstock* (Ed.: M. Aresta), Wiley-VCH, Weinheim, **2010**.
[8] a) B. Loges, A. Boddien, H. Junge, M. Beller, *Angew. Chem. Int. Ed.* **2008**, *47*, 3962; *Angew. Chem.* **2008**, *120*, 4026; b) C. Fellay, P. J. Dyson, G. Laurenczy, *Angew. Chem. Int. Ed.* **2008**, *47*, 3966; *Angew. Chem.* **2008**, *120*, 4030; c) A. Boddien, B. Loges, F. Gärtner, C. Torborg, K. Fumino, H. Junge, R. Ludwig, M. Beller, *J. Am. Chem. Soc.* **2010**, *132*, 8924; d) A. Boddien, D. Mellmann, F. Gärtner, R. Jackstell, H. Junge, P. J. Dyson, G. Laurenczy, R. Ludwig, M. Beller, *Science* **2011**, *333*, 1733; e) J. F. Hull, Y. Himeda, W. H. Wang, B. Hashiguchi, R. Periana, D. J. Szalda, J. T. Muckerman, E. Fujita, *Nat. Chem.* **2012**, *4*, 383; f) E. A. Bielinski, P. O. Lagaditis, Y. Zhang, B. Q. Mercado, C. Würtele, W. H. Bernskoetter, N. Hazari, S. Schneider, *J. Am. Chem. Soc.* **2014**, *136*, 10234.

[9] a) X. Zhou, Y. Huang, W. Xing, C. Liu, J. Liao, T. Lu, *Chem. Commun.* **2008**, 3540; b) M. Ojeda, E. Iglesia, *Angew. Chem. Int. Ed.* **2009**, *48*, 4800; *Angew. Chem.* **2009**, *121*, 4894; c) K. Tedsree, C. W. A. Chan, S. Jones, Q. Cuan, W. K. Li, X. Q. Gong, S. C. E. Tsang, *Science* **2011**, *332*, 224; d) K. Tedsree, T. Li, S. Jones, C. W. A. Chan, K. M. K. Yu, P. A. J. Bagot, E. A. Marquis, G. D. W. Smith, S. C. E. Tsang, *Nat. Nanotechnol.* **2011**, *6*, 302; e) S. Jones, J. Qu, K. Tedsree, X. Q. Gong, S. C. E. Tsang, *Angew. Chem. Int. Ed.* **2012**, *51*, 11275; *Angew. Chem.* **2012**, *124*, 11437; f) X. J. Gu, Z. H. Lu, H. L. Jiang, T. Akita, Q. Xu, *J. Am. Chem. Soc.* **2011**, *133*, 11822; g) Y. Chen, Q. L. Zhu, N. Tsumori, Q. Xu, *J. Am. Chem. Soc.* **2015**, *137*, 106; h) Q. L. Zhu, N. Tsumori, Q. Xu, *J. Am. Chem. Soc.* **2015**, *137*, 11743; i) K. Jiang, K. Xu, S. Zou, W. B. Cai, *J. Am. Chem. Soc.* **2014**, *136*, 4861; j) Y. Y. Cai, X. H. Li, Y. N. Zhang, X. Wei, K. X. Wang, J. S. Chen, *Angew. Chem. Int. Ed.* **2013**, *52*, 11822; *Angew. Chem.* **2013**, *125*, 12038; k) S. Zhang, Ö. Metin, D. Su, S. Sun, *Angew. Chem. Int. Ed.* **2013**, *52*, 3681; *Angew. Chem.* **2013**, *125*, 3769; l) Z. L. Wang, J. M. Yan, Y. Ping, H. L. Wang, W. T. Zheng, Q. Jiang, *Angew. Chem. Int. Ed.* **2013**, *52*, 4406; *Angew. Chem.* **2013**, *125*, 4502; m) Q. Liu, X. Yang, Y. Huang, S. Xu, X. Su, X. Pan, J. Xu, A. Wang, C. Liang, X. Wang, T. Zhang, *Energy Environ. Sci.* **2015**, *8*, 3204.

[10] a) Q. Y. Bi, X. L. Du, Y. M. Liu, Y. Cao, H. Y. He, K. N. Fan, *J. Am. Chem. Soc.* **2012**, *134*, 8926; b) Q. Y. Bi, J. D. Lin, Y. M. Liu, X. L. Du, J. Q. Wang, H. Y. He, Y. Cao, *Angew. Chem. Int. Ed.* **2014**, *53*, 13583; *Angew. Chem.* **2014**, *126*, 13801.

[11] Q. Liu, Y. Duan, Q. Zhao, F. Pan, B. Zhang, J. Zhang, *Langmuir* **2014**, *30*, 8238.

[12] a) H. W. Liang, W. Wei, Z. S. Wu, X. Feng, K. Müllen, *J. Am. Chem. Soc.* **2013**, *135*, 16002; b) W. Niu, L. Li, X. Liu, N. Wang, J. Liu, W. Zhou, Z. Tang, S. Chen, *J. Am. Chem. Soc.* **2015**, *137*, 5555.

[13] a) L. Guo, W. J. Jiang, Y. Zhang, J. S. Hu, Z. D. Wei, L. J. Wan, *ACS Catal.* **2015**, *5*, 2903; b) D. A. Bulushev, M. Zacharska, A. S. Lisitsyn, O. Y. Podyacheva, F. S. Hage, Q. M. Ramasse, U. Bangert, L. G. Bulusheva, *ACS Catal.* **2016**, *6*, 3442.

[14] Note that there was no clear trend of the surface content of pyridinic-N species for this family of CN_x materials, inferring the complex origin of the surface N species. We confirmed in our experiments that, the present chitosan-based pyrolysis approach can realize a homogeneous incorporation of N atoms into the carbon matrix with tunable surface chemistry, simply by varying the combination ratio of chitosan to the N-containing precursors. Among the various materials examined here, $CN_{0.25}$ obtained by pyrolysis of chitosan–urea mixtures affords, by far, the highest surface density of pyridinic-N species.

[15] J. H. Lee, J. Ryu, J. Y. Kim, S. W. Nam, J. H. Han, T. H. Lim, S. Gautam, K. H. Chae, C. W. Yoon, *J. Mater. Chem. A* **2014**, *2*, 9490.

[16] a) A. Boddien, F. Gärtner, C. Federsel, P. Sponholz, D. Mellmann, R. Jackstell, H. Junge, M. Beller, *Angew. Chem. Int. Ed.* **2011**, *50*, 6411; *Angew. Chem.* **2011**, *123*, 6535; b) G. Papp, J. Csorba, G. Laurenczy, F. Joó, *Angew. Chem. Int. Ed.* **2011**, *50*, 10433; *Angew. Chem.* **2011**, *123*, 10617; c) S. F. Hsu, S. Rommel, P. Eversfield, K. Muller, E. Klemm, W. R. Thiel, B. Plietker, *Angew. Chem. Int. Ed.* **2014**, *53*, 7074; *Angew. Chem.* **2014**, *126*, 7194.

[17] A. Bulut, M. Yurderi, Y. Karatas, Z. Say, H. Kivrak, M. Kaya, M. Gulcan, E. Ozensoy, M. Zahmakiran, *ACS Catal.* **2015**, *5*, 6099.

[18] a) D. Preti, C. Resta, S. Squarcialupi, G. Fachinetti, *Angew. Chem. Int. Ed.* **2011**, *50*, 12551; *Angew. Chem.* **2011**, *123*, 12759; b) G. Gao, Y. Jiao, E. R. Waclawik, A. Du, *J. Am. Chem. Soc.* **2016**, *138*, 6292.

[19] a) Y. Maenaka, T. Suenobu, S. Fukuzumi, *Energy Environ. Sci.* **2012**, *5*, 7360; b) A. M. Lilio, M. H. Reineke, C. E. Moore, A. L. Rheingold, M. K. Takase, C. P. Kubiak, *J. Am. Chem. Soc.* **2015**, *137*, 8251.

Received: June 20, 2016
Revised: July 18, 2016
Published online: August 23, 2016

